Heat Transfer Resulting From the Interaction of a Vortex Pair With a Heated Wall

Roland Martin
Laboratoire de Modélisation et d'Imagerie en Géosciences,
CNRS UMR 5212 and INRIA Futurs Magique3D,
Université de Pau et des Pays de l'Adour,
Bâtiment IPRA,
Avenue de l'Université,
64013 Pau, France

Roberto Zenit
Instituto de Investigaciones en Materiales,
Universidad Nacional Autónoma de México,
Apartado Postal 70-360,
Distrito Federal 04510, México

The motion of a two-dimensional vortex pair moving toward a wall is studied numerically. The case for which the wall is heated is analyzed. The equations of momentum and energy conservation are solved using a finite volume scheme. In this manner, the instantaneous heat transfer from the wall is obtained and is related to the dynamics of the fluid vortex interacting with the wall. It was found that, as expected, when the fluid vortex approaches the wall, the heat transfer increases significantly. The heat transfer changes in a nonmonotonic manner as a function of time: When the vortex first reaches the wall, a volume of heated fluid is convected from the wall; this fluid volume circulates in the vicinity of the wall, causing the rate of heat transfer to decrease slightly, to then increase again. A wide range of Prandtl and Reynolds numbers were tested. A measure of the effective heat transfer coefficient, or Nusselt number, is proposed.
[DOI: 10.1115/1.2885182]

Keywords: vortex pair, wall interaction, convective heat transfer, simulation

1 Introduction

Convective heat transfer is probably the most commonly used method to remove heat from a heated source in engineering applications. The nature of the fluid flow is, hence, the factor that determines how effective the heat removal is. In spite of its prominence, the design of convective heat transfer devices has been mainly empiric. To be able to further enhance the convective heat transfer processes, the details of the interaction between fluid flow and walls have to be fully understood.

Clearly, the fluid motion over a wall has a direct implication to the heat transfer rate, as heat is convected by the flow. Although the understanding of convective heat transfer is very well developed for the case of steady flows, the determination of unsteady heat transfer coefficients is still incipient [1]. Understanding such unsteady processes is a key factor to achieve the increasing need of fast heat removal from modern engineering applications. In particular, the unsteady motion created by vortices and its implications to the increase of heat transfer [2] is of significant importance: One of the most common techniques to enhance the convective heat transfer uses vortex generators (see, for example, Refs. [3,4] and references therein). As vortices interact with walls, an unsteady boundary layer develops, which has direct implications to the rate of heat transfer [5,6].

The interaction of vortical structures with walls has been analyzed by many authors in a variety of configurations [7]. Of particular interest, because of its apparent simplicity, is the case of a compact isolated vortex ring impinging normally over a solid wall [8]. The evolution of this flow configuration is complex: Resulting from the vortex fluid motion, an unsteady boundary layer develops on the wall. The vorticity created on the wall is convected, resulting in the formation of a secondary vortex, which interacts with the original one. These two vortical structures continue to interact with each other, creating, in some cases, a third vortex. These observations were originally obtained by experiments [8,9], but were also verified by numerical simulations [10,11].

For the case of nonisothermal flows, most investigations have been focused to understand the effect of vortical structures over the global heat transfer rate. Studies of the effect of an isolated vortex are less common. Reulet et al. [12] investigated the effect of an isolated vortex, produced by a flapping wing, convected by a turbulent stream over a heated wall. They found that the evolution of the thermal boundary layer was strongly coupled with the dynamic effects of the vortex. Romero-Méndez et al. [13] analytically calculated the effects of isolated Rankine vortices over walls in different configurations and found that in all cases an increase of the heat transfer was observed. Although this study considered an idealized flow, it gave a significant insight on the fundamental processes that occur during the interaction of vortices with walls and their implications with heat transfer.

The objective of this paper is to study the mechanism by which heat is removed from a wall resulting from the interaction of a coherent vortical structure. A simplified arrangement has been chosen to solve this problem: the normal impingement of a 2D vortex pair with a flat heated wall. We have opted to use computer simulations to be able to study the sole effect of the coherent fluid flow on the wall heat flux. An experimental study of the same problem would have an additional important complication: Natural convection would always be present; therefore, it would not be possible to study the removal of heat without this effect. The case for which both vortical motion and natural convection contribute to the rate of heat transfer could be of interest, in particular, for practical applications; however, its study lies beyond the current investigation.

Using a modified SIMPLE numerical scheme, the equations of momentum and energy are solved to find the velocity and temperature fields as a function of time. The instantaneous heat transfer from the wall is calculated and related to the motion of the fluid in the vicinity of the wall. The heat transfer rates are correlated to the convective and diffusive processes at the moment of impact of the vortex at the wall and for long periods. We first introduce the general mathematical formulation of the problem; then, the problem of study is described. The numerical method and its implementation issues are then discussed. The results are presented and discussed.

Contributed by the Heat Transfer Division of ASME for publication in the JOURNAL OF HEAT TRANSFER. Manuscript received December 4, 2006; final manuscript received July 2, 2007; published online April 8, 2008. Review conducted by Gautam Biswas.

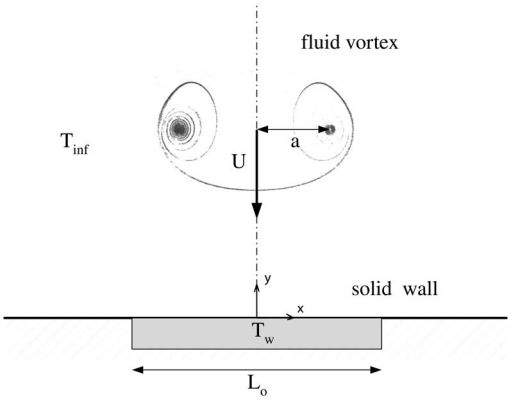

Fig. 1 The interaction of a vortex pair (or ring) with a heated wall

2 Mathematical Formulation

The flow studied here is two dimensional, unsteady, laminar, and incompressible. The dimensionless conservation equations are the continuity

$$\nabla \cdot \mathbf{u}^* = 0 \tag{1}$$

time-dependent momentum

$$\frac{\partial \mathbf{u}^*}{\partial t^*} + (\mathbf{u}^* \cdot \nabla^*)\mathbf{u}^* + \nabla^* P^* = \frac{1}{\mathrm{Re}} \nabla^{*2} \mathbf{u}^* \tag{2}$$

and energy conservation

$$\frac{\partial T^*}{\partial t^*} + (\mathbf{u}^* \cdot \nabla^*)T^* = \frac{1}{\mathrm{RePr}} \nabla^{*2} T^* \tag{3}$$

where $\mathbf{u}^* = (u^*, v^*)$ is the 2D velocity field with components in $x^* = x/a$ (horizontal) and $y^* = y/a$ (vertical), $P^* = P/\rho U^2$ is the pressure, and $t^* = t/(a/U)$ is the dimensionless time. U and a are the characteristic velocity and distance, respectively. The Reynolds number Re is defined as $\mathrm{Re} = Ua/\nu$, where ν is the kinematic viscosity. For the case of interest, a is the size of the vortex pair (defined as the initial distance between the centers of the two rectilinear vortices) and U its displacement velocity. The Prandtl number is defined as $\mathrm{Pr} = \nu/\alpha$, where α is the thermal diffusivity.

The energy equation is formulated in a nonconservative form in order to decouple it from the momentum conservation equation. The fluid is assumed to be Newtonian with constant properties. Re and Pr vary, respectively, in ranges of 250–1000 and 0.7–100 in order to investigate their influence on the heat transfer of a vortex impinging with an isothermal wall. No-slip and constant temperature conditions are considered for all walls. A segment of the lower wall (over which the vortex pair impinges) is kept at a higher constant temperature. At each time step, the temperature is computed in the computational domain and the heat flux is calculated over the heated region.

3 Problem Definition

In this investigation, the interaction of a vortex pair with a heated wall is studied. A 2D configuration is considered: a pair of counter-rotating equal-strength vortices moving at the same velocity toward a fixed heated wall. Particularly, we focus on evaluating the enhancement of the heat transfer resulting from this interaction.

The problem under investigation is depicted schematically in Fig. 1. A vortex pair (the equivalent of a vortex ring in 3D) is placed at an initial distance of $4a$ from a solid wall. The distance between the centers of the two rectilinear vortices is $2a$. The center of the pair moves initially at a velocity U in a trajectory perpendicular to the wall (y direction). At the center of the bottom solid wall, a plate of length L_o is kept at a fixed temperature T_w. The fluid is contained between four solid walls of length L. The size of the square domain is such that $L = 4L_o$. The fluid and the walls, with the exception of the heated plate, are initially at the same temperature, T_{inf}.

The initial condition of the simulation considers a 2D cut of a Hill spherical vortex [14]. This configuration allows us to directly relate the translational velocity of the pair with its size (separation distance between centers). For such a vortical structure, the vorticity is confined into the interior of a uniformly translating cylinder of radius a. The vortex lines form circles about an axis passing through the center of the disk and the streamlines lie in meridional planes. Outside the disk, the flow is irrotational. After some manipulations [15], the velocity is given by an inviscid irrotational formulation derived from a scalar function Ψ expressed as

$$\Psi = \begin{cases} \dfrac{15U}{20a^2}\left(x^4 + x^2y^2 + \dfrac{5}{3}x^2a^2\right) & \text{for } x^2 + y^2 < a^2 \\ \dfrac{Ua^3}{2}x^2(x^2 + y^2)^{-3/2} & \text{for } x^2 + y^2 > a^2 \end{cases} \tag{4}$$

where U is the translation velocity of the vortex in the y direction. Clearly, for this case $u = -\partial\Psi/\partial y$ and $u = \partial\Psi/\partial x$. Note that the coordinate system is taken to be at the center of the vortex. From Eq. (4), it is easily verified that the irrotational motion for $x^2 + y^2 > a^2$ is also described by the velocity potential

$$\Phi = -\frac{Ua^3}{2}\frac{y}{(x^2 + y^2)^{3/2}} \tag{5}$$

which is the potential function of a rigid disk moving through an ideal fluid with a y velocity U.

The initial pressure field is

$$P = P_{\mathrm{inf}} - \rho\frac{U^2a^3}{2}\left(\frac{x^2 - 2y^2}{(x^2 + y^2)^{3/2}} + \frac{a^3(x^2 + 4y^2)}{x(x^2 + y^2)^4}\right), \quad x^2 + y^2 > a^2 \tag{6}$$

Taking into account the continuity of pressure across the surface of the disk, we find

$$P = H - \rho|\mathbf{u}|^2, \quad x^2 + y^2 < a^2 \tag{7}$$

where H is the Bernoulli constant,

$$H = \frac{25U^2}{40a^2}x^2(x^2 + y^2)$$

and

$$\rho|\mathbf{u}|^2 = \frac{9U^2}{4a^4}\left(y^2x^2 + y^2(y^2 + x^2)^2 + \frac{a^2y^2}{9}\right)$$

This inviscid vortex is taken solely as the initial condition to start the numerical simulation of the problem. Clearly, as the full Navier–Stokes equations are solved in time, this condition adapts itself to that of a viscous pair moving toward a wall. Note also that this initial condition does not account for the presence of the wall.

The temperature of the vortex is initially set to be the same as the ambient temperature of the flow. The temperature of the heated patch on the wall is maintained constant and higher than the flow temperature by 45 K. The length of the isothermal plate is given by L_0. The heat flux over the isothermal heated plate is evaluated.

4 Numerical Method

In the present study, a finite volume technique is used, considering a SIMPLE-like method. For more details, the reader is referred to Ref. [16]. A linearization and an alternating direction implicit (ADI) decomposition of the momentum equations are introduced to ensure a second order and semi-implicit time stepping

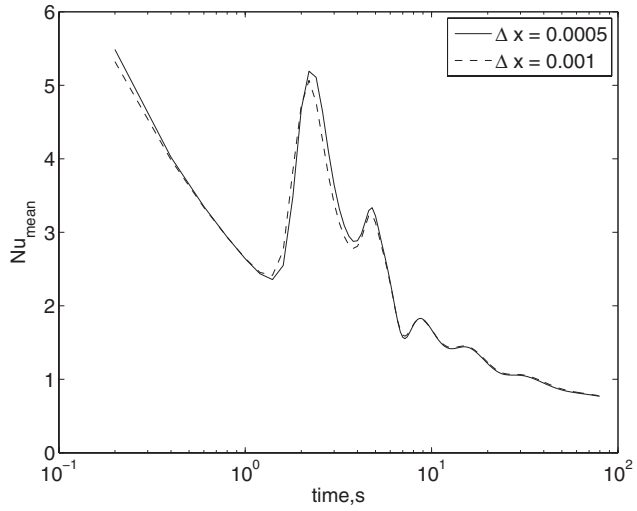

Fig. 2 Mean Nusselt number as a function of time. Simulations for two mesh sizes, considering Re=250 and Pr=0.7.

formulation of the predictor step and a semi-implicit formulation of the predictor step [17]. At each ADI step, a tridiagonal linear system is solved. A second/third order monotone upwind scheme for conservation laws (MUSCL) flux limiter is also introduced in the formulations of the convective fluxes to reduce the numerical diffusion. In the corrector step, a convergence criterion for the pressure correction algorithm is implemented to ensure a mass residual less than or equal to 10^{-4}. Then, the energy equation is solved by computing the temperature in an iterative procedure ensuring a 10^{-7} temperature accuracy. Antisymmetric conditions are implemented for velocities at the walls. Different mesh sizes were tested, and it was found that the numerical dispersion disappears for meshes of 200×200 with a mesh size of 0.0005. In all the simulations, the courant number is taken as $\max(U_{\max}\Delta t/\Delta x, \mu\Delta t/\Delta x^2)\leqslant 0.2$. The simulations with these mesh sizes and time steps, as will be shown in the next section, are in good agreement with other previously reported numerical results. Figure 2 shows the calculated mean Nusselt number (see the definition in Eq. (10)) for a typical flow, for two different values of the mesh size. Clearly, the results are grid independent.

Many different combinations of Reynolds and Prandtl numbers were studied. The Reynolds number ranged from 250 to 1000 to study laminar-inertial flows. The Prandtl number was varied from 1.4 to 13.3. These range of values corresponds to the physical properties of most common liquids. A few additional simulations were also performed with Prandtl numbers of 0.7 and 100 (considering only Re=250 and 1000) to cover the physical properties corresponding to gases and oils, respectively.

All the computations were performed for several characteristic time scales $t_{\text{char}}=a/U$, up to the order 15 (corresponding to approximately 50 s). Such calculations consist of approximately 500,000 time steps, corresponding to approximately 150 CPU min in a personal computer (3 GHz, Pentium IV processor). Computations are performed with the same small time step of 0.0005 s and a grid resolution of 200×200 for the same mesh size of 0.0005 m.

The physical properties of water are considered for all the calculations. The values of the thermal diffusivity α are varied artificially to achieve several values of Pr. Different values of Re are obtained, varying only the magnitude of U, keeping the relative size of the vortex (with respect to the container) fixed.

5 Results

5.1 Flow Field. Figure 3 shows the evolution of the vorticity field as the vortical structure approaches and reaches the wall. Since, for the case studied here, the flow remains symmetric, only the fields on the right side are shown. For all cases, as explained above, the energy and momentum equations are uncoupled. Hence, the isothermal velocity field is first resolved. Each image shows the vorticity field for a different time instant; additionally, isovorticity lines are shown to facilitate the identification of the vortical structures. Before the vortex pair reaches the wall ($t^*=t/(a/U)\leqslant 1$), the vorticity is confined within the vortex core. This is expected since a Hill vortex structure was chosen as the initial condition. When the vortex moves closer to the wall ($t^*=1.5$), the forced fluid motion over the wall creates an unsteady boundary layer ($t^*=2$). The boundary layer separates as a result of the flow-induced adverse pressure gradient. The vorticity created during the separation detaches from the wall, forming a secondary vortex ($t^*=2.5$). The primary and secondary vortices interact with each other and the wall ($2.5<t^*<4.5$). The formation of tertiary vortex can be observed for larger Re cases. The fluid motion is eventually dissipated by the effect of viscosity. The figure shows only the results for Re=250. Other simulations, for higher values of the Re, show a similar behavior.

The motion of the vortices obtained with our computer simulations can be compared with the analytical results of two counter-rotating inviscid vortices interacting with a wall. The solution of this classical problem can be found in Ref. [18]. The trajectory of the center of the vortex is given by

$$4x^2y^2 = C(x^2+y^2) \tag{8}$$

where C is an arbitrary constant that depends on the initial separation of the vortex pair (a in our case). It is interesting to note that this analytical result is independent of the circulation of the vortex pair. Figure 4 shows a comparison of the prediction of Eq. (8) and the trajectories of the center of the vortices for two different values of Re. Clearly, away from the wall, the trajectories of the simulated vortex pair are in good agreement with the inviscid theory, corresponding to times $t^*<1.5$. However, as expected, as the vortex approaches the wall, the trajectory of the vortex pair is greatly affected. From Fig. 3, it can be observed that for $t^*>1.5$, there is a significant amount of vorticity being produced at the wall; hence, the inviscid prediction is not expected to be accurate.

The rich flow physics of a viscous vortex pair (or ring) interacting with a solid wall has been reported before by several authors (see, for example, Ref. [8]). In particular, to quantitatively validate our results, a comparison with the results of Orlandi [10] is presented, who simulated the interaction of a vortex pair with a wall; as opposed to our simulations, he considered the case for which the distance between the centers of the vortices and the translation speed were independent. The trajectory of the main vortex obtained by Orlandi is shown also in Fig. 4. Despite the fact that the simulation conditions are not identical, the agreement between these results is good.

5.2 Evolution of Temperature Field. Figure 5 shows the evolution of the temperature field for the same flow shown in Fig. 3, considering a value of Pr=1.4. As in the previous figure, isovorticity lines are also shown on top of the temperature fields. When the simulation starts, the temperature of the fluid is lower than that of the plate. Even before the vortical structure reaches the wall, the heat from the plate has begun to diffuse into the fluid ($t^*=1$). When the vortex moves closer and interacts with the wall ($t^*=1.5$), heat is strongly convected away from the wall by the motion of the fluid ($1.5<t^*<3$). Subsequently, as a result of the recirculating nature of the fluid motion, the heated lump of fluid returns back to the wall ($3.5<t^*<4$), resulting in a decrease of

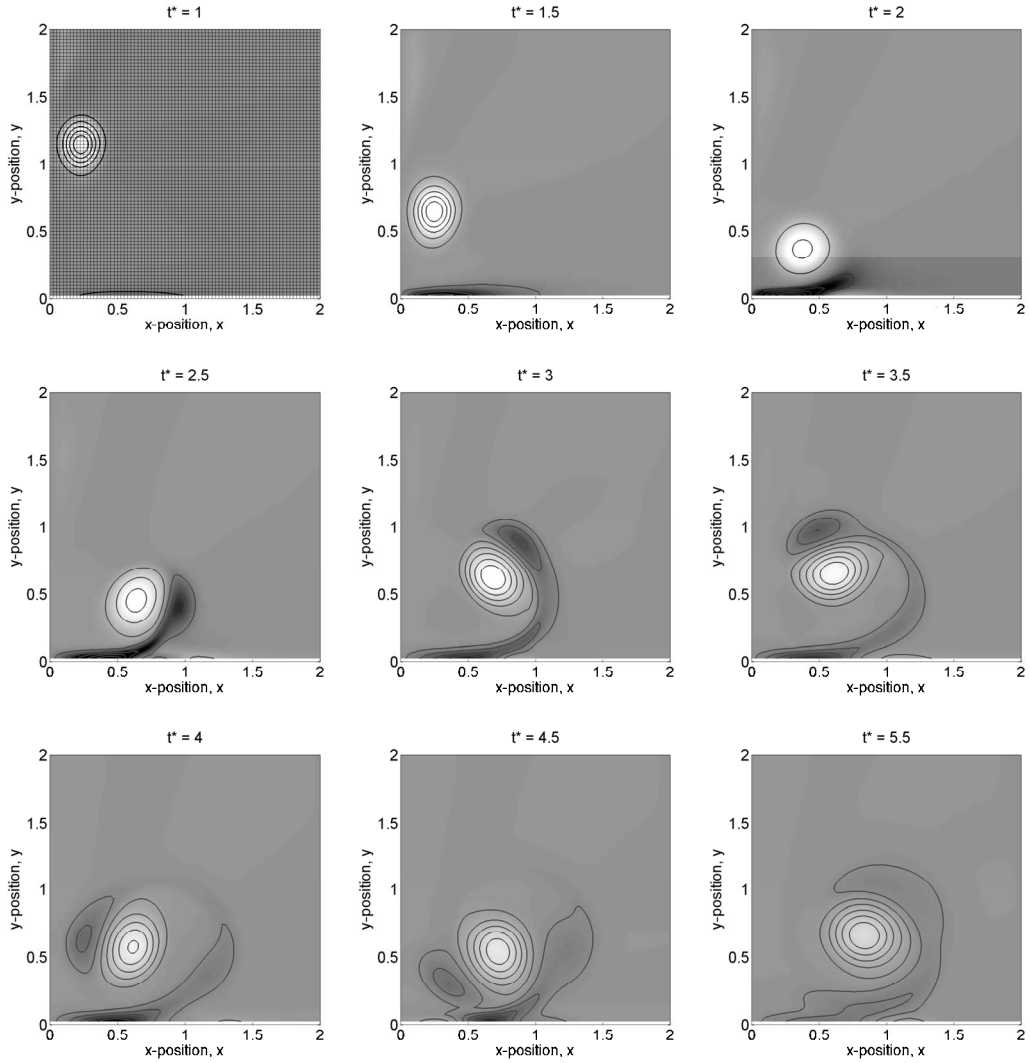

Fig. 3 Evolution of the vorticity field. Black and white levels on the figure represent values of 0.5 s^{-1} and −0.5 s^{-1} of vorticity, respectively. The solid lines show contours of isovorticity, which are used to visualize the vortical structures. The case shown is for Re=250. The time is shown in dimensionless terms: $t^*=t/(a/U)$. A unit of t^* represents the time it takes for a vortex to move, at a constant velocity U, a distance equivalent to its size. The distances are normalized by the size of the heated plate: x/L_0 and y/L_0. Note that only the right side of the simulation is shown. The mesh shown on the first image is indicative of the computational grid.

the rate of heat transfer. However, along with the heated fluid, a fresh volume of fluid is also dragged over the wall, resulting in a second increase of the heat transfer ($t^*=4.5$). The rate of heat transfer continues to decrease for subsequent times. Many simulations were conducted for a wide range of Re and Pr; a similar qualitative behavior was observed for all cases.

5.3 Wall Heat Transfer. The local wall heat transfer can be expressed in dimensionless terms as

$$\mathrm{Nu}=\frac{h(x)L_0}{k}=\frac{L_0\left.\dfrac{\partial T}{\partial y}\right|_{y=0}}{T_w-T_{\inf}} \tag{9}$$

where T_w is the temperature at the wall, $T_{\inf}$ is the initial temperature of the fluid away from the wall, L_0 is the length of the heated plate, k is the thermal conductivity of the liquid, and $h(x)$ is the local convective heat transfer coefficient.

Figure 6 shows the value of the local Nusselt number as a function of the horizontal coordinate over the length of the wall, for the simulation results shown in Figs. 3 and 5. Each line represents the dimensionless heat transfer for different instants during the interaction of the vortex with the wall. Clearly, the heat transfer increases to a maximum value when the vortex pair reaches the wall, which occurs at $t^*=2$, for that particular value of Re. Also, it is interesting to note that for most times, the Nusselt number is relatively uniform across the plate. This uniformity results from the fact that the size of the vortex pair is comparable to the size of the heated plate. Nevertheless, there is a variation of the heat transfer over the plate; therefore, to quantify the total heat transfer resulting from the vortex-wall interaction, the mean averaged Nusselt number over the heated wall can be calculated as

$$\mathrm{Nu}_{\mathrm{mean}}=\frac{1}{L_0}\int_{-L_0/2}^{L_0/2}\frac{h(x)x}{k}dx \tag{10}$$

where the local convective heat transfer coefficient $h(x)$ is defined as

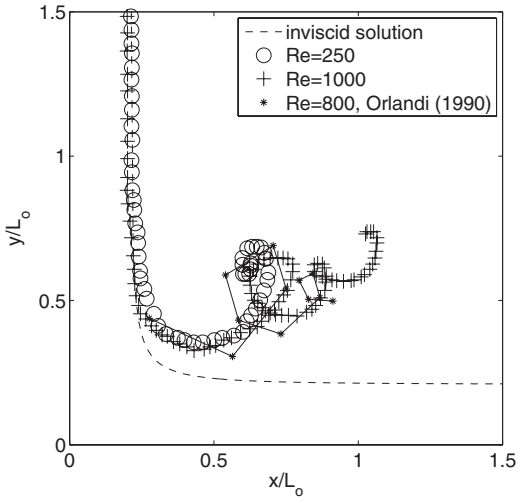

Fig. 4 Trajectory of the center of the main vortex. Two simulation cases are shown: (○) Re=250; (+) Re=1000. The dashed line is the trajectory from Eq. (8), considering C=22.9. The results of Orlandi [10] are also shown.

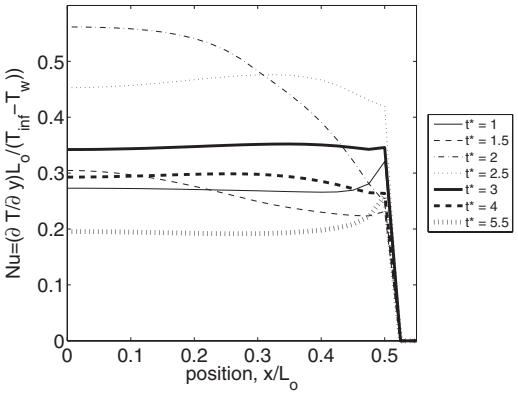

Fig. 6 Nusselt number as a function of position over the plate for different time instants. The case shown is for Re=250 and Pr=1.4. Note that only the right side of the profile is shown.

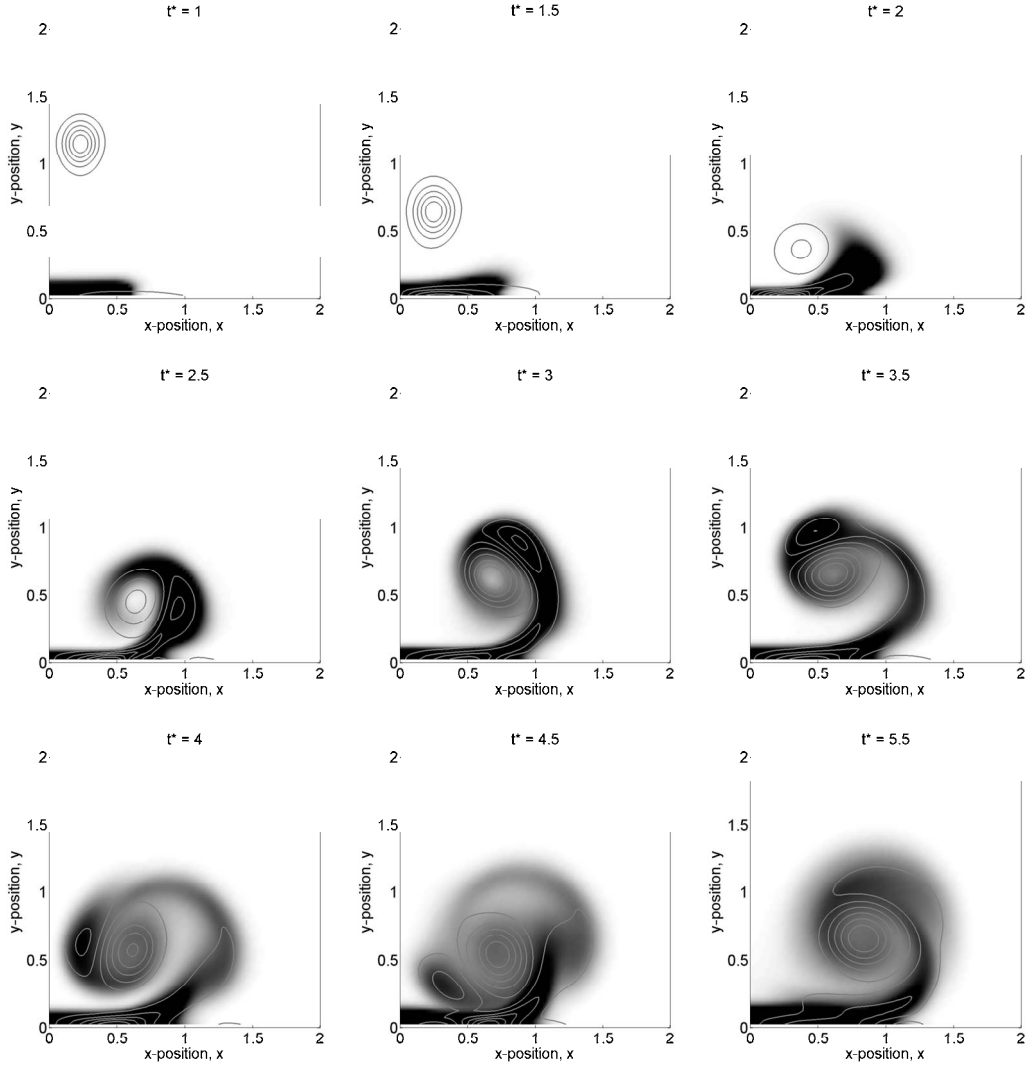

Fig. 5 Evolution of the temperature field. Black and white levels in the figure represent values of 0.9 and 1.0 of the dimensionless temperature $(T-T_w)/(T_{inf}-T_w)$, respectively. The solid lines show contours of isovorticity, which are used to visualize the vortical structures. The case shown is for Re=250 and Pr=1.4. Time and size are scaled, as in Fig. 3. Note also that only the right side of the simulation is shown.

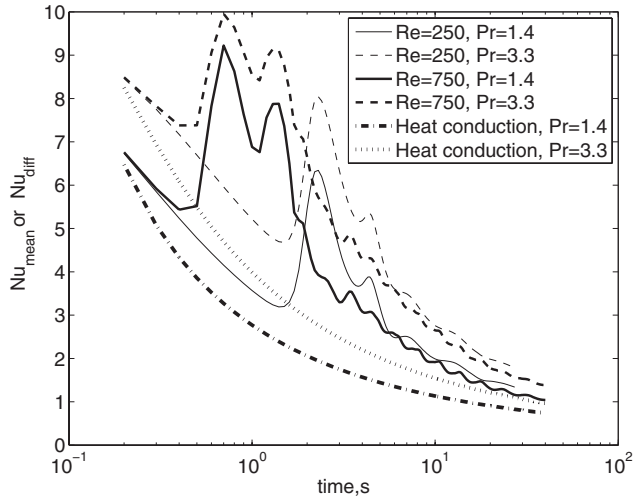

Fig. 7 Mean Nusselt number as a function of time. Simulations for two typical values of Re and Pr are shown. Also, simulations for a purely conductive system (no fluid motion) are shown for comparison.

$$h(x) = \frac{k}{T_w - T_{\inf}} \left(\frac{\partial T}{\partial y}\right)\bigg|_{y=0} \tag{11}$$

Figure 7 shows results for four typical simulations, where the mean Nusselt number Nu_{mean} is shown as a function of time. One of the cases shown (Re=250, Pr=1.4) corresponds to the simulation results shown in Figs. 3 and 5. Clearly, for early times, the Nusselt number decreases as a function of time as the heat from the wall is being diffused mainly by conduction through the fluid. When the fluid vortex approaches the wall, a sudden increase of the heat transfer is observed. The heat transfer then decreases as a result of the recirculating nature of the flow; a second increase of the Nusselt number can be observed, but with a smaller magnitude than the first. For the cases shown in the figure, the purely conductive, Nu_{diff}, solution was calculated to serve as a basis of comparison. The purely diffusive heat transfer coefficient is obtained from the solution of the same geometry considering no fluid motion; that is, $(u^*, v^*) = (0, 0)$ everywhere in the computational domain. The heat transfer for the purely conductive case is below the vortex-convected case. Hence, the enhancement of the rate of heat removal from the wall results from the interaction of the vortical structure with the wall. The same qualitative behavior is observed in all the cases shown in the figure. Figure 8 shows the calculated value of the Nusselt number by first varying the value of Pr for the same Re (a) and vice versa (b). As the Reynolds number increases, the peak of heat transfer appears earlier because the vortex pair moves faster and reaches the wall sooner. Also, the magnitude of the peak is larger for larger Re. Moreover, as the Prandtl number increases, the heat transfer also increases. Hence, for this case, the heat transfer is dominated by the convective action of the fluid motion.

5.4 Enhancement of Heat Transfer. To evaluate the amount of additional heat transferred resulting from the interaction of the vortex pair with the wall, the ratio of the vortex induced heat transfer (Nu_{mean}) and that for the purely conductive case (Nu_{diff}) is calculated. Figure 9 shows the ratio Nu_{mean}/Nu_{diff} as a function of time for several characteristic values of the Reynolds and Prandtl numbers. It can be clearly observed that during the interaction of the vortex with the wall, the heat transfer can be enhanced as much as 3.2 times the value corresponding to the conductive case. The heat transfer enhancement increases with Re and Pr.

To obtain a quantitative measurement of the enhancement, we locate the maximum value Nu_{max} of the heat transfer achieved

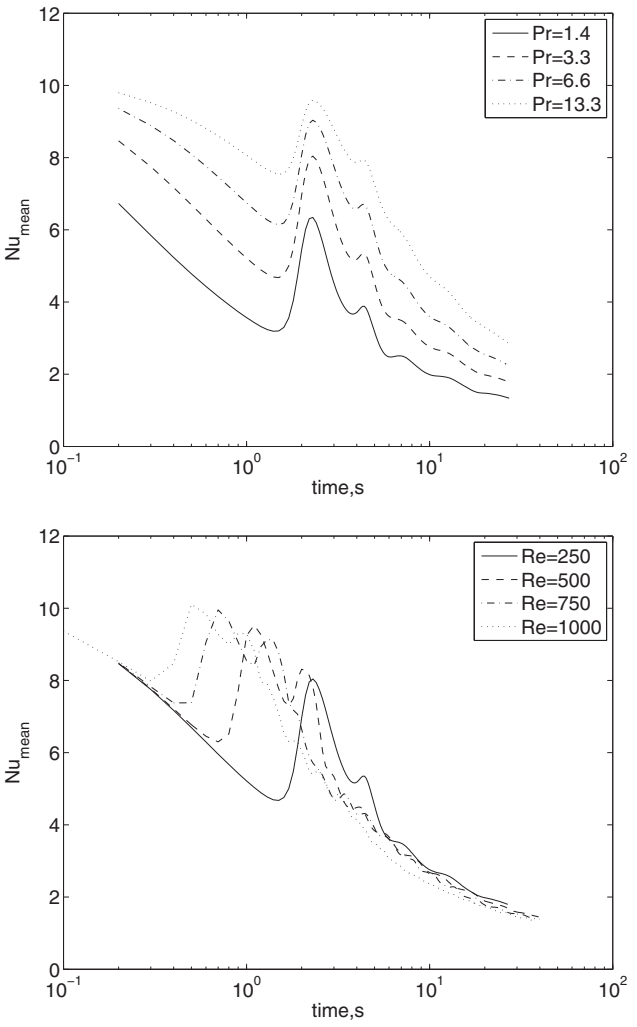

Fig. 8 Mean Nusselt number as a function of time. (*a*) Simulations keeping Re fixed and Pr varied. (*b*) Simulations keeping Pr fixed and Re varied.

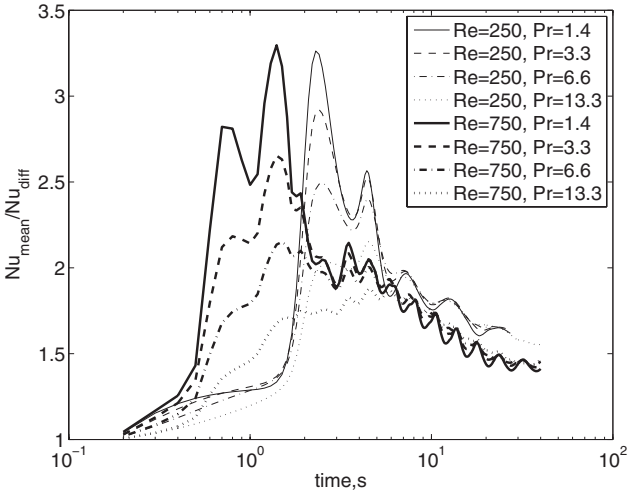

Fig. 9 Ratio of the mean convective to the purely conductive Nusselt numbers. Simulations for two typical Re numbers are shown for four values of Pr.

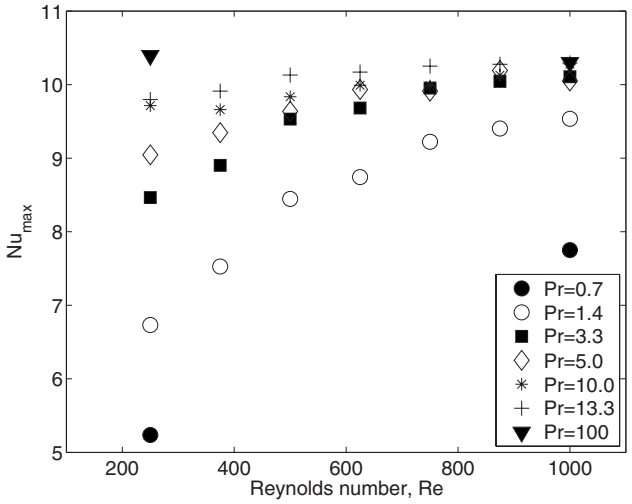

Fig. 10 Maximum of the mean Nusselt number against the Reynolds number for several values of Pr between 1.4 and 13.26. Additional results are also shown for Pr=0.7 and 100 and for Re=250 and 1000.

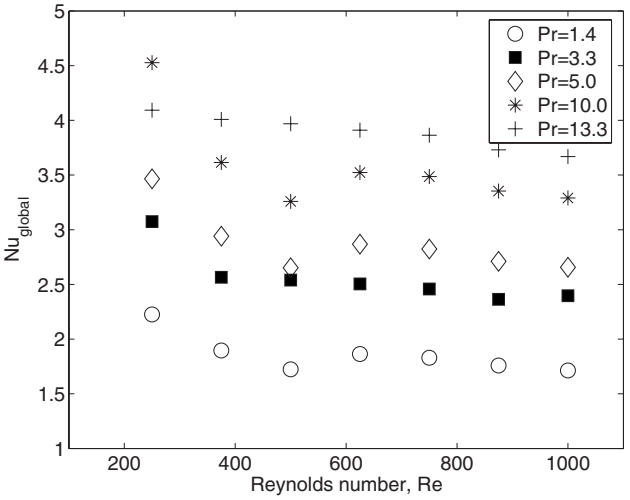

Fig. 11 Time integral of the mean Nusselt number against the Reynolds number for several values of Pr between 1.4 and 13.26

during the interaction. This value corresponds to the time instant at which the vortex first interacts with the wall. Figure 10 shows the value of Nu_{max} as a function of the flow Reynolds number for a range of values of the Prandtl number. For all cases, the value of the maximum heat transfer increases with Re hence, the enhancement of heat transfer increases with the Reynolds number. The results also show that the maximum heat transfer increases with Pr, as the Prandtl number increases, the dependence with the Reynolds number becomes less important. The results presented in the figure can be fitted to the following expression:

$$Nu_{max} = 4.139 Re^{0.113} Pr^{0.076} \tag{12}$$

This equation, however, is not very accurate for certain values of the Pr and Re since it assumes a dependence of the type $Re^{\alpha}Pr^{\beta}$, where α and β are constants. A better fit of the numerical results can be given by the relation

$$Nu_{max} = 27.68 Re^{0.0206}(1 - Pr^{-0.1265}) Re^{0.3221/Pr} \tag{13}$$

This expression is more accurate than formula (12), but only for the range of parameters chosen in this investigation. Moreover, from equations like this, the functional dependence of the independent variable is not evident at first sight, and its physical meaning is not obvious.

The maximum value of the Nusselt number is clearly not the only significant parameter to quantify the enhancement of heat transfer resulting from the interaction of the vortex pair with the wall. As it has been shown above, there is a complex nonsteady fluid-wall interaction that results in continuous changes in the value of the heat transfer rate. To obtain a global measurement of the heat transfer resulting from this interaction, a time averaged Nusselt number can be calculated as

$$Nu_{global} = \frac{1}{T}\int_0^T Nu_{mean}(t)dt$$

where T is the total time during which the interaction is significant. Figure 11 shows the *global* Nusselt number as a function of Re for several values of Pr. This average value of the heat transfer coefficient decays slightly with the Reynolds number and increases with the value of the Prandtl number. By averaging over a long time, the unsteady effects of the flow are lumped into Nu_{global}, and the global heat removal is determined mainly by the fluid thermal properties; hence, one may expect a weak dependence on the flow Reynolds number considering this measure of the effective heat transfer.

Note that some variability can be observed in these measurements; this is the result of the choice of the averaging time T used in the calculations. For some combinations of Re and Pr, the duration of the interaction is very long. For practical reasons, most simulations were stopped at $t_{char}=15$ (corresponding to approximately 50 s or approximately 500,000 time steps). Despite this variability, the general trend in the results is very clear.

6 Conclusions

In this investigation, the motion of a vortex pair impinging on a solid wall was studied. The fluid motion that resulted from this interaction causes an increase of the local heat transfer coefficient. Although it is clear that a forced fluid motion over a heated wall causes an increase of the heat transfer from the wall, the details of the process had not yet been investigated to date. In particular, the case of the interaction of an isolated vortex pair (or ring) with a heated wall had not been previously reported.

Our isothermal simulations were in good agreement with previously reported experimental and numerical results. The collision of a vortex pair with a flat wall results in a complex fluid-wall interaction that has direct implications to the rate of heat transfer.

The simulations showed that the heat transfer increases as a result of the vortex-wall interaction, compared to the purely conductive case. The heat transfer reaches a maximum value when the vortex first arrives at the wall, to then decrease as the flow continues to develop and a secondary vortex forms; subsequently, the heat transfer reaches a second local maximum value when the fluid, pushed by the circulating heated lump, is forced to interact with the wall. Several local maxima, of decaying relative magnitude, were observed at a frequency that is proportional to the vortex circulation. The magnitude of the heat transfer rate increases with the values of the Reynolds and Prandtl numbers.

References

[1] Goldstein, R. J., Eckert, E. R. G., Ibele, W. E., Patankar, S. V., Simon, T. W., Kuehn, T. H., Strykowski, P. J., Tamma, K. K., Bar-Cohen, A., Heberlein, J. V. R., Davidson, J. M., Bischof, J., Kulacki, F. A., Kortshagen, U., Garrick, S., and Srinivasan, V., 2005, "Heat Transfer: A Review of 2002 Literature," Int. J. Heat Mass Transfer, **48**, pp. 819–927.

[2] Fiebig, M., 1997, "Vortices and Heat Transfer," Z. Angew. Math. Mech., **77**, pp. 3–18.

[3] Valencia, A., and Sen, M., 2003, "Unsteady Flow and Heat Transfer in Plane Channels With Spatially Periodic Vortex Generators," Int. J. Heat Mass Transfer, **46**, pp. 3189–3199.

[4] Yang, S.-J., 2003, "Numerical Study of Heat Transfer Enhancement in a Chan-

nel Flow Using an Oscillating Vortex Generator," Heat Mass Transfer, **39**, pp. 257–265.
[5] Doligalski, T. L., and Walker, J. D. A., 1984, "The Boundary Layer Induced by a Convected Two-Dimensional Vortex," J. Fluid Mech., **139**, pp. 1–28.
[6] Escriva, X., and Giovannini, A., 2003, "Analysis of Convective Momentum and Wall Heat Transfer: Application to Vortex Boundary Layer Interaction," Int. J. Heat Mass Transfer, **46**, pp. 2471–2483.
[7] Doligalski, T. L., Smith, C. R., and Walker, J. D. A., 1994, "Vortex Interactions With Walls," Annu. Rev. Fluid Mech., **26**, pp. 573–616.
[8] Walker, J. D. A., Smith, C. R., Cerra, A. W., and Doligalski, T. L., 1987, "The Impact of a Vortex Ring on a Wall," J. Fluid Mech., **181**, pp. 99–140.
[9] Ersoy, S., and Walker, J. D. A., 1986, "Flow Induced at a Wall by a Vortex Pair," AIAA J., **24** (10), pp. 1597–1605.
[10] Orlandi, P., 1990, "Vortex Dipole Rebound From a Wall," Phys. Fluids A, **2**, pp. 1429–1436.
[11] Chang, T. Y., Hertzberg, J. R., and Kerr, R., M., 1997, "Three-Dimensional Vortex/Wall Interaction: Entrainment in Numerical Simulation Experiment," Phys. Fluids, **9**(1), pp. 57–66.
[12] Reulet, P., Marchand, M., and Millan, P., 1998, "Experimental Characterization of the Convective Vortex-Wall Interaction," Rev. Gen. Therm., **37**(8), pp. 661–668.
[13] Romero-Méndez, R., Sen, M., Yang, K. T., and McClain, R. L., 1998, "Enhancement of Heat Transfer in an Inviscid-Flow Thermal Boundary Layer Due to a Rankine Vortex," Int. J. Heat Mass Transfer, **41**, pp. 3829–3840.
[14] Hill, M. J. M., 1894, "On a Spherical Vortex," Philos. Trans. R. Soc. London, Ser. A, **185**, pp. 213–245.
[15] Saffman, P. G., 2001, *Vortex Dynamics*, Cambridge University Press, Cambridge, England.
[16] Patankar, S. V., 1980, *Numerical Heat Transfer and Fluid Flow*, Hemisphere, New York.
[17] Van Doormal, J. P., and Raithby, G. D., 1984, "Enhancements of the SIMPLE Method for Predicting Incompressible Fluid Flows," Numer. Heat Transfer, **7**, pp. 147–163.
[18] Lamb, H., 1995, *Hydrodynamics*, Cambridge University Press, New York..